

The human CENP-A centromeric nucleosome-associated complex

Daniel R. Foltz^{1,3}, Lars E. T. Jansen^{1,3}, Ben E. Black^{1,3}, Aaron O. Bailey⁴, John R. Yates III⁴ and Don W. Cleveland^{1,2,3,5}

The basic element for chromosome inheritance, the centromere, is epigenetically determined in mammals. The prime candidate for specifying centromere identity is the array of nucleosomes assembled with CENP-A, the centromere-specific histone H3 variant. Here, we show that CENP-A nucleosomes directly recruit a proximal CENP-A nucleosome associated complex (NAC) comprised of three new human centromere proteins (CENP-M, CENP-N and CENP-T), along with CENP-U(50), CENP-C and CENP-H. Assembly of the CENP-A NAC at centromeres is dependent on CENP-M, CENP-N and CENP-T. Facilitates chromatin transcription (FACT) and nucleophosmin-1 (previously implicated in transcriptional chromatin remodelling and as a multifunctional nuclear chaperone, respectively) are absent from histone H3-containing nucleosomes, but are stably recruited to CENP-A nucleosomes independent of CENP-A NAC. Seven new CENP-A-nucleosome distal (CAD) centromere components (CENP-K, CENP-L, CENP-O, CENP-P, CENP-Q, CENP-R and CENP-S) are identified as assembling on the CENP-A NAC. The CENP-A NAC is essential, as disruption of the complex causes errors of chromosome alignment and segregation that preclude cell survival despite continued centromere-derived mitotic checkpoint signalling.

The centromere is a specialized chromatin domain present throughout the cell cycle that acts as a platform on which the transient assembly of the kinetochore occurs during mitosis^{1,2}. The kinetochore mediates the attachment of spindle microtubules and unattached kinetochores regulate progression of mitosis through the mitotic (or spindle assembly) checkpoint. Human centromeres are comprised of a complex assembly of simple repeated DNA sequences including 0.3–5 megabases of alphoid DNA¹. Nevertheless, neither this, nor any other DNA sequence, is necessary or sufficient for centromere specification as new centromeres (referred to as neocentromeres) are known to arise at chromosomal loci that have no sequence similarity to canonical centromeres, and centromeres can be inactivated despite apparently intact DNA sequences³. This has led to the belief that centromeres are specified epigenetically.

All active centromeres are characterized by the presence of long arrays of nucleosomes in which CENP-A replaces histone H3^{1,4,5}. DNA stretching has revealed that these CENP-A nucleosomes are interspersed with those carrying histone H3 (ref. 6). As the element most proximal to DNA, identification of centromeres could be achieved by assembly of functionally distinct CENP-A-containing, centromere-specific, nucleosomes as an epigenetic mark. Consistent with this possibility, a subnucleosomal heterotetramer of CENP-A and histone H4 exists that has a uniquely rigid conformation (relative to the corresponding heterotetramer of histones H3 and H4)⁷ induced by the CENP-A targeting domain (CATD) of CENP-A. The process

by which CENP-A is incorporated into centromeric DNA, and the factors responsible, are not known.

Unlike yeast, where the molecular architecture of the centromere has been extensively defined^{8,9}, the molecular complexes that link the mammalian CENP-A nucleosome to the many other components of the centromere (those components that are stably associated across the cell-cycle and those transiently associated in mitosis) are not known. Essential constitutive centromere components include CENP-A¹⁰, CENP-C (or Mif2 in budding yeast)^{11,12}, CENP-I (or Mis6 in fission yeast)^{13–16}, CENP-H¹⁷ and Mis12 (ref. 13), which are required for the recruitment of many constitutive centromere components, as well as transient kinetochore components that are involved in generating and sensing microtubule attachment^{15–19}. Previous studies using immunoprecipitation with a CENP-A antibody to enrich arrays of up to 30 human CENP-A-containing nucleosomes identified 41 associated proteins, 37 of which were previously unknown potential human centromere components²⁰. However, only two were confirmed as *bona fide* centromere constituents and no functional properties were examined. For the remaining 35, it is not known whether any are selectively recruited to CENP-A nucleosomes.

Using multiple tandem affinity purifications (TAPs), we now define the most proximal complex directly recruited by CENP-A-containing centromeric nucleosomes, CENP-A NAC, and a set of seven CAD components recruited to centromeric nucleosomes through their interaction with CENP-A NAC.

¹Ludwig Institute for Cancer Research and Departments of ²Medicine and ³Cellular and Molecular Medicine, University of California at San Diego, La Jolla, CA 92093–0670, USA. ⁴The Scripps Research Institute, La Jolla, CA 92037, USA.

⁵Correspondence should be addressed to D.W.C. (e-mail: dcleveland@ucsd.edu)

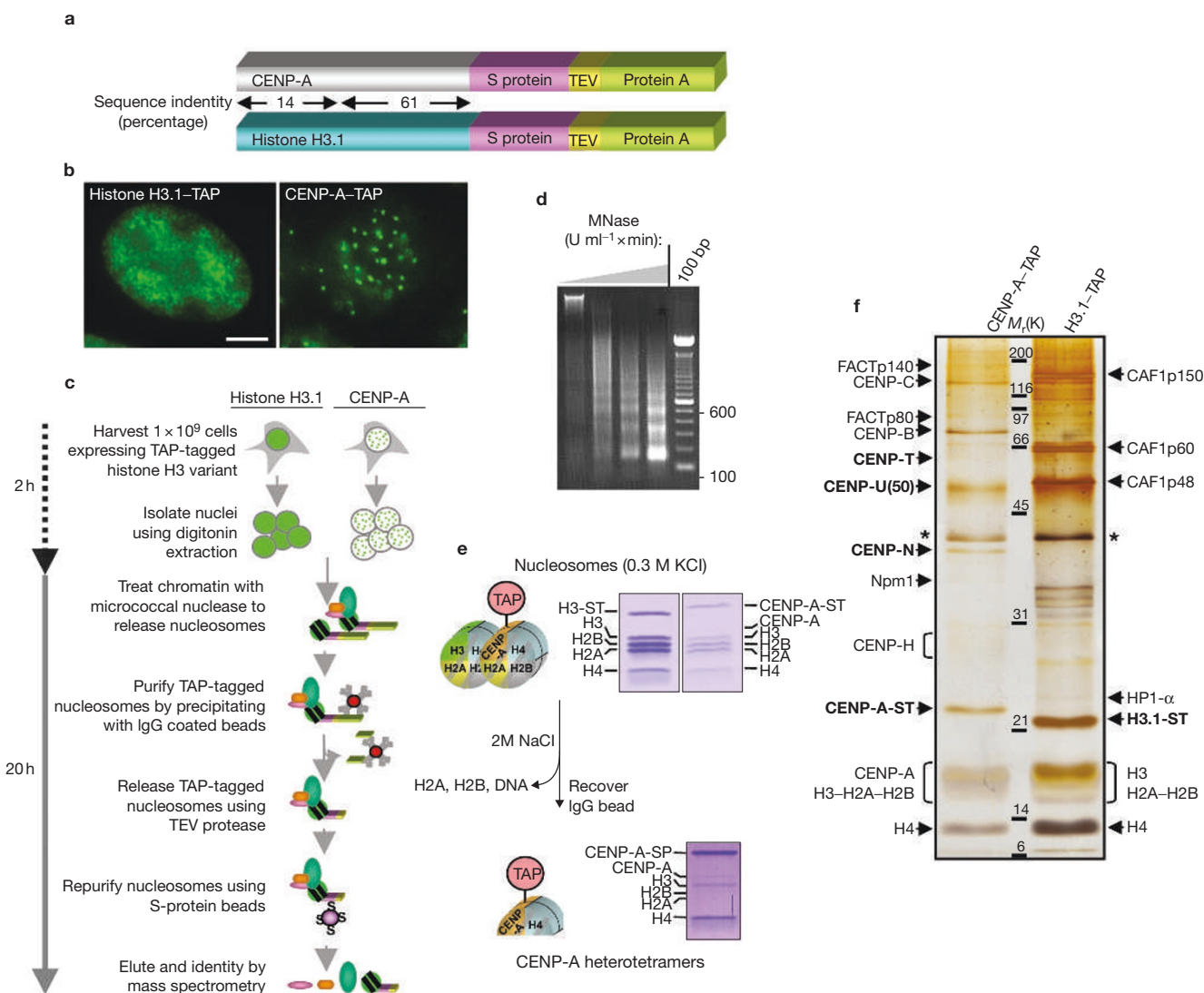


Figure 1 Purification of CENP-A nucleosomes. **(a)** TAP tags consisting of S-protein and protein A tags separated by a TEV protease site were fused to the C-termini of CENP-A and histone H3.1. The percentage amino acid identity between the CENP-A and histone H3.1 amino termini and histone fold domains are shown. **(b)** Stable cell lines expressing either histone H3.1-TAP or CENP-A-TAP were established. Localization of histone H3.1-TAP and CENP-A-TAP constructs was assessed by immunocytochemistry using FITC conjugated rabbit IgG. The scale bar represents 5 μm . **(c)** Strategy for tandem affinity purification of TAP-tagged nucleosomes by micrococcal nuclease (MNase) production of a soluble nucleosome pool derived from a nuclear fraction. **(d)** DNA isolated from

nucleosomes produced by micrococcal nuclease digestion. **(e)** Isolation of DNA-free, subnucleosomal heterotetramers of CENP-A produced by high salt treatment of CENP-A nucleosomes and affinity recovery of CENP-A-TAP. Polypeptide composition (top) of the initial CENP-A-TAP or H3.1-TAP nucleosomes or the CENP-A heterotetramers (bottom) visualized by Coomassie blue staining. **(f)** Eluates from tandem affinity purifications of CENP-A and histone H3.1 containing nucleosomes were separated by SDS-PAGE and visualized by silver staining. ST indicates the location of the TAP tagged constructs. Asterisks indicate a contaminating protein. Proteins were identified based on mass spectrometry results combined with predicted molecular weights.

RESULTS

Purification of centromeric CENP-A nucleosome arrays

Multiple stable HeLa cell lines expressing either carboxy (C)-terminal TAP-tagged²¹ CENP-A or histone H3.1 (Fig. 1a, b) were established. CENP-A-TAP incorporated into centromeric loci (Fig. 1b), indicating that the fusion protein retained functional properties of endogenous CENP-A. Moreover, increased levels of tagged CENP-A reduced accumulation of endogenous CENP-A (see Supplementary Information, Fig. S1a, b), consistent with competition of exogenous CENP-A for assembly at endogenous centromeres. Histone H3.1-TAP showed the diffuse nuclear localization (Fig. 1b) that was expected for incorporation into non-centromeric chromatin.

CENP-A or histone H3.1-containing nucleosomes were tandem affinity purified (Fig. 1c) from a soluble pool of mainly mononucleosomes (with a minority of larger species containing 2–4 nucleosomes; Fig. 1d). As expected, Coomassie blue staining of histone H3.1 nucleosomes revealed an approximate 1:1:1:1 ratio of the core histones (H2A, H2B, H3 and H4; Fig. 1e). This is consistent with the isolation of histone octamers derived from intact chromatin, as opposed to a predominance of the H3.1:H4 heterotetramers representing prenucleosomal complexes^{22,23}.

Almost equimolar levels of CENP-A-TAP and histones H2A, H2B and H4 were found in the CENP-A-TAP nucleosomes (Fig. 1e). Although CENP-A nucleosomes have been proposed to be homotypic with respect to the histone H3 variant they incorporate^{6,24}, a polypeptide of the size

Table 1 Composition of CENP-A–TAP and histone H3.1–TAP nucleosomes determined by mass spectrometry

CENP-A–TAP				Histone H3.1–TAP			
	M_r (K)	Spectrum count	Coverage (percentage)		M_r (K)	Spectrum count	Coverage (percentage)
Chromatin remodelling factors and nuclear chaperones				Chromatin-assembly factors			
FACTp140	140	103	14	CAF1p150	150	409	15
FACTp80	80	81	12	CAF1p60	60	440	17
hFLEG1	54	81	13	CAF1p48	52	12	7
Npm1	33	67	19	CAF1p46	48	32	5
Known centromere proteins				Chromatin-binding proteins			
CENP-B	65	93	25	HP1- α	22	15	29
CENP-C	107	456	32	HP1- β	21	45	31
CENP-H	28	14	25	BANF1	10	3	27
CENP-U(50)	47	23	18				
Novel centromere proteins							
CENP-M	20	14	6				
CENP-N	40	51	21				
CENP-T	60	14	8				
Nucleosome				Nucleosome			
CENP-A	16	6	12	Histone H3	15	8	20
Histone H3	15	3	14	Histone H2A	14	442	39
Histone H2A	14	1846	37	Histone H2B	14	254	12
Histone H2B	14	989	32	Histone H4	12	129	40
Histone H4	12	1551	57	Histone H1	10	12	25
Histone H1	10	88	15				

of histone H3 was present at approximately 60% the level of CENP-A in the CENP-A nucleosomes (Fig. 1e) and this was confirmed by mass spectrometry (Table 1). Histone H3 present in the CENP-A nucleosomes may reflect the presence of H3-containing nucleosomes interspersed within arrays of centromeric CENP-A nucleosomes⁶ or heterotypic nucleosomes containing one molecule of CENP-A and one molecule of histone H3 (along with two molecules of histone H4). CENP-A nucleosomes were disrupted with 2 M NaCl (known to dissociate H2A, H2B and the DNA from the H3:H4 heterotetramer)²⁵ and components still bound to CENP-A were recovered (Fig. 1e). As expected, H2A and H2B were dissociated completely, whereas CENP-A and H4 were retained. Nevertheless, a significant proportion (15%) of the initial histone H3 also remained (Fig. 1e), consistent with a minority of the initial nucleosomes containing both histone H3 and CENP-A — presumably in heterotypic tetramers with two histone H4 molecules.

Purified CENP-A–TAP and histone H3.1–TAP nucleosome complexes contained almost completely distinct non-histone components (Fig. 1f, Table 1 and see Supplementary Information, Fig. S1c). For CENP-A nucleosomes, these included the previously known centromere proteins CENP-B, CENP-C, CENP-H and CENP-U(50). The presence of these known centromere proteins (including CENP-B, which is localized to centromeres by DNA sequence specific binding to the CENP-B box²⁶) in the CENP-A nucleosomes, but not the histone H3 nucleosomes verified that CENP-A–TAP nucleosomes are functionally integrated into endogenous centromeres.

Chromatin assembly factors (CAFs) stably associate exclusively with histone H3.1 nucleosomes

Assembly of the histone H3.1 nucleosome is dependent on a complex of CAFs which include CAF1p150, CAF1p60, CAF1p48 (also known

as RbAp48) and CAF1p46 (also known as RbAp46)²⁷. The CAF-1 complex associates with prenucleosomal heterotetramers containing the DNA replication-dependent H3.1 variant²², but not with histone H3.3 heterotetramers²⁸. The histone H3.1 complexes isolated here not only contained substantial levels of the heterochromatin binding proteins HP1- α and HP1- β ²⁹, but also components of CAF-1 (including CAF1p150, CAF1p60, CAF1p48 and CAF1p46; Fig. 1f and Table 1). None of these components were detected in CENP-A–TAP nucleosomes. Thus, in addition to being part of the prenucleosomal complex, a proportion of CAF-1 is also a stably-bound component of H3.1-containing chromatin.

Histone H2A.Z and macroH2A enrichment in CENP-A nucleosomes

Nucleosomes containing distinct histone H2A variants have been implicated in unique functional processes including gene expression (macroH2A and H2A.Z) and DNA repair (H2A.X)^{4,30}. Although most peptides are common to all of the H2A variants, and were found at comparable frequencies in the CENP-A and histone H3.1 nucleosomes (Table 2), two peptides uniquely identifying H2A.Z and six identifying the macroH2A variant were enriched in the CENP-A nucleosomes when compared with those containing histone H3.1. This is consistent with their enrichment in CENP-A nucleosomes or the neighboring histone H3 containing nucleosomes. However, H2A.X was under-represented in the CENP-A nucleosomes.

Identification of the CENP-A NAC

Uniquely associated with the CENP-A nucleosomes were CENP-U(50) (previously named MLF1IP³¹ and CENP-50; ref. 32) and a set of three proteins CENP-M³³, CENP-N and CENP-T (Fig. 1f, Table 1 and see

Table 2 Summary of peptides unique to histone H2A variants found in CENP-A and histone H3.1 nucleosomes by mass spectrometry

Histone variant	CENP-A-TAP		Histone H3.1-TAP	
	Peptides	Number of spectra	Peptides	Number of spectra
Histone H2A.X	LLGGVTIAQGGVLPNIQAVLLPK	4	LLGGVTIAQGGVLPNIQAVLLPK	29
	LLGGVTIAQGGVLPNIQAV	5	GVITIAQGGVLPNIQAVLLPK	62
Histone H2A.Z	GDEELDSLIIK	19	GDEELDSLIIK	3
	ATIAGGGVIPH	15	VGATAAVYSAAILEYLTAEVLELAGNASK	3
Histone H2A.Y-macroH2A	SIAFPSIGSGR	103	NGPLEVAGAAVSAGHGLPAK	11
	AASADSTTEGTPADGFTVLSTK	160	AASADSTTEGTPADGFTVLSTK	1
	AGVIFPVGR	4	GKLEAITPPPAK	18
	AISSYFVSTMSSSIK	7		
	EFVEAVLELR	12		
	LEAITPPPAK	10		

Supplementary Information, Table S1). The latter three were among the 41 components previously reported to be present with CENP-A after a single affinity purification²⁰, but none of these have yet been confirmed as authentic centromere components. Homologues of CENP-M and CENP-N are present in other vertebrates (see Supplementary Information, Fig. S2), but each lacks sequence motifs that suggest functional properties.

Expression of each of these putative centromere components as a fusion protein with a localization and purification (LAP)³⁴ tag (consisting of an S protein tag, a TEV (tobacco etch virus) protease site and GFP) revealed that CENP-M, CENP-N, CENP-T and CENP-U(50) were all *bona fide* centromere proteins — each protein was bound to the centromere throughout interphase and during mitosis (Fig. 2a–d). Despite the presence of CENP-B-containing alphoid DNA distributed across the inner centromere³⁵, CENP-A, and all of the newly identified centromere components, were restricted to the outer aspects of each pair of sister centromeres (Fig. 2e). Subsequent affinity purifications to identify the binding partners of CENP-M, CENP-N or CENP-U(50), in which each protein was copurified with each of the others (see Fig. 3), led to the conclusion that CENP-M, CENP-N, CENP-T and CENP-U(50), together with the previously identified centromere components CENP-C³⁶ and CENP-H³⁷, comprise a CENP-A proximal nucleosome associated complex (CENP-A NAC) at human centromeres.

Also present in the purifications of CENP-A nucleosomes, but not the corresponding H3.1 nucleosomes, were a set of proteins that had previously been characterized for their functions in addition to centromere structure. These include the FACT complex components, FACTp140 and FACTp80 (also known as SUPT16H and SSRP1, respectively), that were previously implicated in transcription through chromatinized DNA³⁸, and nucleophosmin-1, a primarily nucleolar protein that had previously been implicated in numerous functions, including as a nuclear molecular chaperone³⁹ and in centrosome duplication⁴⁰.

The components found to be associated with CENP-A nucleosomes may be recruited to centromeric loci through interaction with specific DNA sequences (as is the case for CENP-B) or by the centromere specific CENP-A nucleosome. The dependence of these components on CENP-A for their localization was assessed by reducing CENP-A levels by small hairpin (sh) RNA⁴¹. Depletion of CENP-A had no effect on the localization of the direct sequence binding protein CENP-B (Fig. 2f), but eliminated centromere bound CENP-H — similar to what has been reported in chicken cells⁴². Loading of the newly identified CENP-M and CENP-N was similarly CENP-A dependent (Fig. 2f).

The CENP-A NAC complex recruits a set of CADs

Double affinity purification from cell lines that stably expressed LAP-tagged CENP-M, CENP-N or CENP-U(50) (see Fig. 2) yielded the CENP-A NAC complex that was comprised of CENP-M, CENP-N, CENP-U(50) and CENP-T, together with CENP-C and CENP-H (Fig. 3a, b). This establishes these components as part of a stable centromeric complex that is recruited to CENP-A-containing nucleosomes. CENP-B, human fetal liver expressing gene 1 (hFLEG1), nucleophosmin-1 and the FACT complex members that were initially found to associate with the CENP-A nucleosome (Fig. 1f and Table 1) were absent in these subsequent purifications, confirming that they are not tightly associated with the CENP-A NAC.

Six additional components (CENP-I, CENP-K, CENP-L, CENP-O, CENP-P and CENP-Q) were also purified with each of the CENP-M, CENP-N and CENP-U(50)-containing complexes, indicative of a set of CAD-constitutive centromere components (Fig. 3a, b). Two others (CENP-R and CENP-S) were associated with the CENP-M and CENP-U(50) complexes. CENP-O, CENP-P, CENP-R and CENP-S were each verified as centromere components by expression of LAP-tagged constructs in HeLa cells (Fig. 3c). CENP-K, CENP-L and CENP-Q have been shown by others to be constitutively associated with centromeres (Okada *et al.*, see note added in proof). None of these CAD components directly associated with the CENP-A nucleosome (Fig. 1f and Table 1), demonstrating that they are centromere associated through their interaction with one or more components of the CENP-A NAC.

The presence of varying levels of the constitutive CENPs (Fig. 3a) established a probable hierarchy of interactions. CENP-K and CENP-I seem to be very closely associated with the CENP-A NAC as these proteins show the highest levels in both mass spectrometry and direct silver staining from purification of CENP-M and CENP-N (Fig. 3a, b). CENP-R and CENP-S were identified by mass spectrometry, but were not visible by silver staining and were present in highest relative abundance (based on the peptide coverage) with CENP-M complexes.

CENP-M, CENP-N and CENP-T are required for proper assembly of the CENP-A NAC

The presence of CENP-M, CENP-N, CENP-U(50) and CENP-T, together with CENP-C and CENP-H, in each double affinity purification strongly supports the idea that these proteins assemble into a single CENP-A NAC complex that has direct affinity for the CENP-A nucleosome. Small interference RNA (siRNA)-mediated depletion of these components

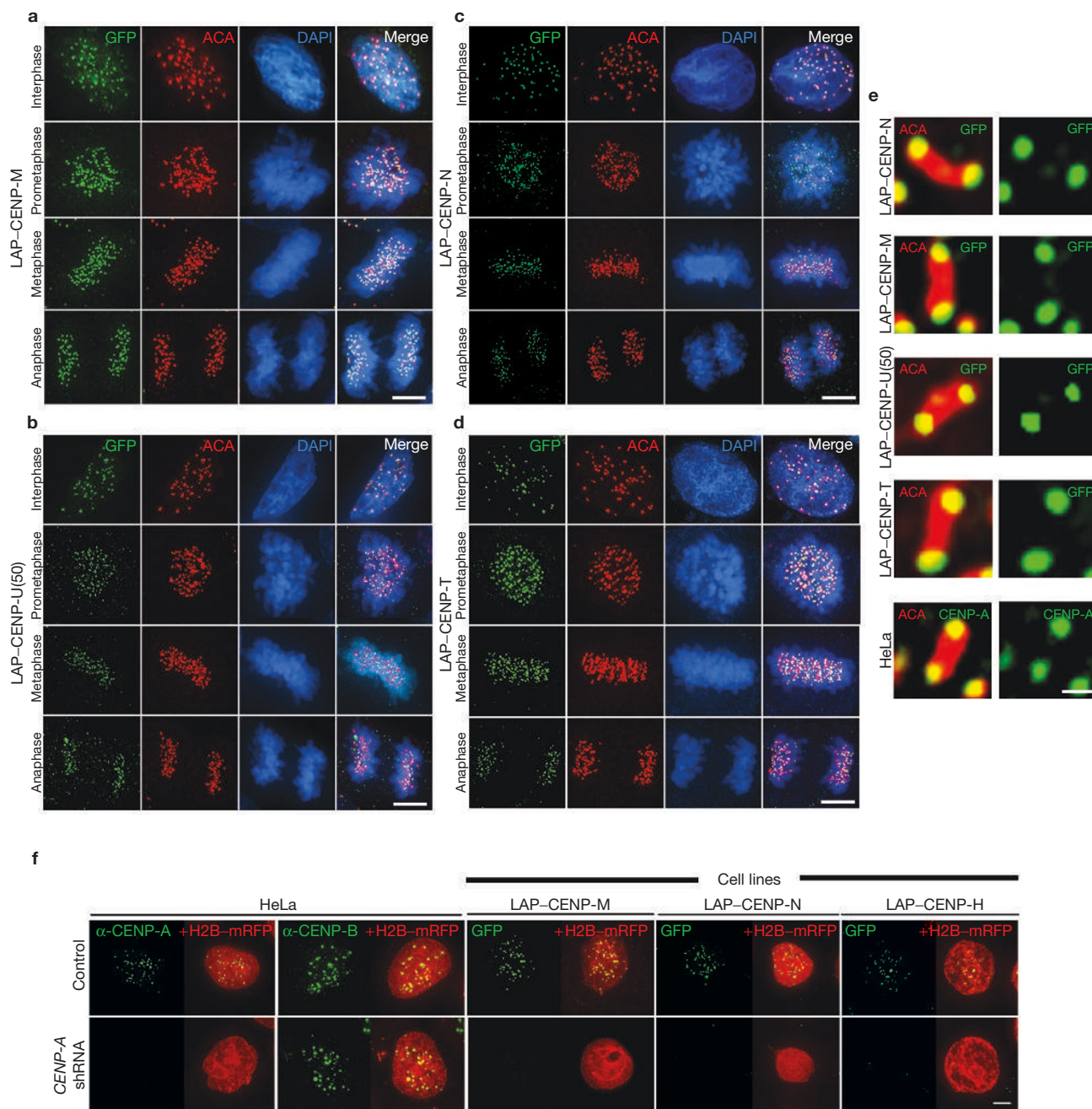


Figure 2 CENP-A dependent centromere localization of four CENP-A nucleosome associated proteins. (a–e) Localization of CENP-A NAC components after establishing HeLa cell lines stably expressing amino terminal LAP-tagged fusions of CENP-M (a), CENP-N (b) and CENP-U(50) (c), or transiently expressing LAP-tagged CENP-T (d). Centromeres detected by an anti-centromere autoimmune serum (ACA; red) that recognizes CENP-A, CENP-B and CENP-C; LAP-tagged fusion proteins localized using anti-GFP antibody (green); and DNA visualized using DAPI (blue). The scale bar

represents 5 μ m. (e) Insets showing high magnification of sister kinetochores during mitosis from images in panels a–d, and also stained for CENP-B to visualize the inner centromere region. CENP-A was localized in HeLa cells using a monoclonal CENP-A antibody. The scale bar represents 0.5 μ m. (f) Decreased centromere loading of LAP-CENP-M, LAP-CENP-N or LAP-CENP-H, but not CENP-B, after shRNA mediated reduction in endogenous CENP-A. H2B-mRFP was co-transfected with the shRNA to identify cells with reduced CENP-A. The scale bar represent 5 μ m.

(see Supplementary Information, Fig. S3a) was used to test whether centromere association of each protein is dependent on formation of this complex. Suppression of *CENP-M*, *CENP-N* or *CENP-T* by siRNA disrupted recruitment of the CENP-A NAC. Reduction of *CENP-M* or *CENP-N* resulted in the loss of the other from centromeres (Fig. 4a, b), as well as the loss of CENP-H (Fig. 4c). Reduction of *CENP-T* eliminated CENP-M at centromeres (Fig. 4a), and presumably CENP-N and CENP-H as these are lost in the absence of *CENP-M* (Fig. 4b, c).

Loss of *CENP-U(50)* produces errors in chromosome attachment without affecting mitotic checkpoint signalling

The dependency of CAD components for binding to the CENP-A NAC was determined using shRNA to eliminate detectable LAP-CENP-U(50) (Fig. 4d) and endogenous *CENP-U(50)* mRNA levels (see Supplementary Information, Fig. S3a). Reduction of *CENP-U(50)* did not affect centromeric recruitment of CENP-A, CENP-B (see Supplementary Information, Fig. S3b), Hec1, CENP-E, CENP-F, Mis12 or Aurora B (data not shown),

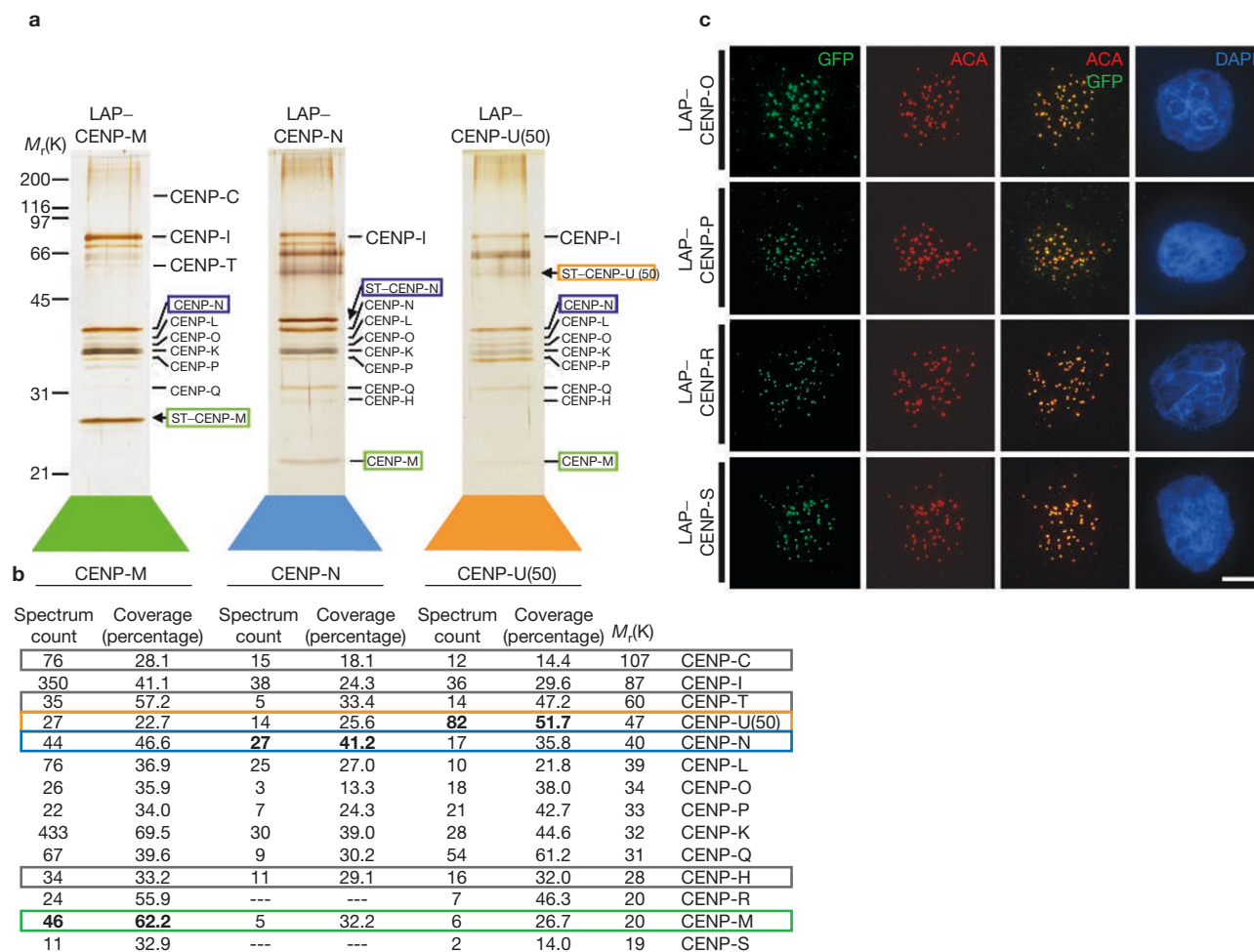


Figure 3 Purification of the CENP-A NAC and identification of its associated CAD complex components. (a) Complexes containing CENP-M, CENP-N and CENP-U(50) were identified by tandem affinity purifications (conducted as in Fig. 1) using anti-GFP and S-tag affinity steps from HeLa cell lines stably expressing LAP-CENP-M, LAP-CENP-N or LAP-CENP-U(50). Purified complexes were separated by SDS-PAGE and proteins were visualized by silver staining. ST (S-tag) indicates the location of the tagged components.

or components of the CENP-A NAC including CENP-H, CENP-M and CENP-N (Fig. 4d). However, it eliminated LAP-tagged CENP-O and CENP-P from interphase (Fig. 4d) and mitotic centromeres (data not shown), establishing that their loading requires CENP-U(50).

A primary function of the centromere-kinetochore is to prevent chromosome missegregation through generation by unattached kinetochores of a mitotic (or spindle assembly) checkpoint inhibitor that blocks premature advance to anaphase¹. To determine whether centromeres depleted of CENP-U(50) retained the capacity to generate this inhibitory signal, microtubule assembly was blocked with nocodazole in cells depleted of CENP-U(50) with shRNA. Under these conditions, normal cells accumulate in mitosis with each unattached kinetochore generating a maximal inhibitory signal. As similar proportions of normal and CENP-U(50)-depleted cells arrested with 4N DNA contents (Fig. 5a), CENP-U(50), and the components it recruits, are not required either for activating or sustaining mitotic checkpoint activity, at least under conditions in which a maximal signal (when all kinetochores are unattached) would normally be generated.

Live cell time-lapse imaging of CENP-U(50)-depleted cells (Fig. 5b) revealed mitotic errors (occurring in 45% of mitoses). The most

(b) Mass spectrometry was used to identify the components in each purified fraction. Components also found in CENP-A-TAP nucleosome purifications are boxed. Spectrum count and coverage values for tagged proteins are in bold. (c) HeLa cells stably expressing CENP-O or CENP-P or transiently expressing LAP-CENP-R or LAP-CENP-S were immunostained using anti-GFP antibodies (green), ACA (red) to detect centromeres and DAPI (blue) to detect DNA. The scale bar represents 5 μ m.

prominent errors included delay in anaphase onset (Fig. 5c) and the presence of lagging chromosomes during pseudometaphase and anaphase (Fig. 5b,d,e and see Supplementary Information, Movies 1, 2). Another 10% of CENP-U(50)-depleted cells entered anaphase with misaligned chromosomes, and approximately 20% sustained a prolonged arrest with unaligned chromosomes. Cells depleted of CENP-U(50) that escaped mitotic arrest usually failed to complete chromosome alignment before onset of anaphase (Fig. 5e).

The variety of defects observed (including the occurrence of cells that progress through mitosis with lagging and misaligned chromosomes despite extended pre-anaphase) were indicative of microtubule-kinetochore interactions that were persistently unstable, even after satisfaction of the mitotic checkpoint. To directly assess the generation of the mitotic checkpoint inhibitor at individual CENP-U(50) depleted centromeres, recruitment of an eYFP-tagged version of mitotic checkpoint inhibitor, mitotic-arrest deficient 1 (eYFP-Mad1), which is bound to kinetochores and released after stable microtubule capture^{43,44}, was determined by live cell microscopy (Fig. 5f). Depletion of CENP-U(50) produced kinetochores that recruited levels of Mad1 that were comparable with control

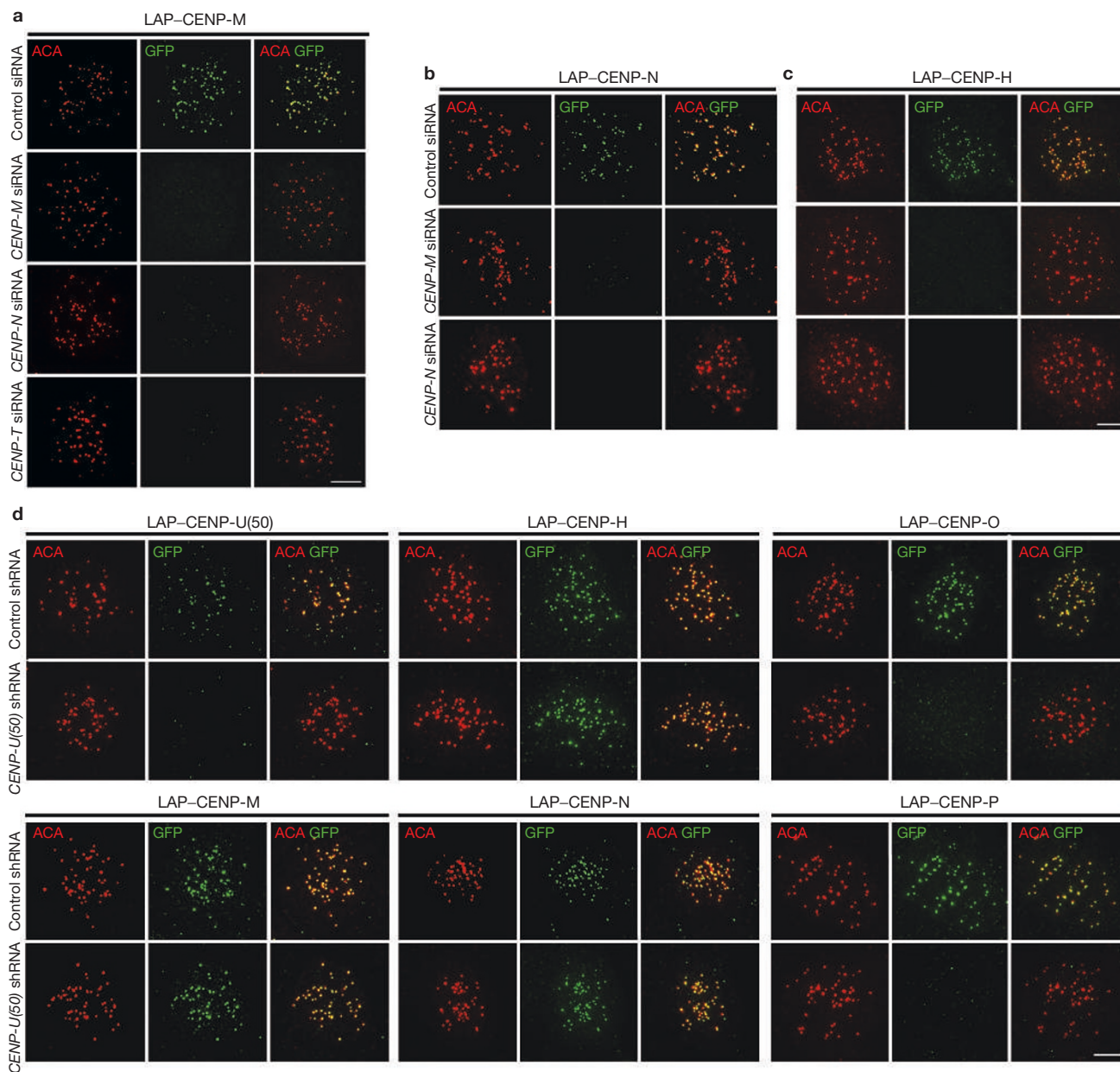


Figure 4 Assembly of the CENP-A NAC requires CENP-M and CENP-N. (a–c) Integrity of the CENP-A NAC was determined after reduction of CENP-M, CENP-N or CENP-T levels using transfection of the corresponding siRNAs into cells expressing LAP-CENP-M (a), LAP-CENP-N (b) or LAP-CENP-H (c). (a) Reduction of the indicated CENP-A NAC components eliminated centromeric localization of CENP-M. (b) CENP-N loading at kinetochores required CENP-M. (c) CENP-H loading required both CENP-M and CENP-N. (d) Transcription mediated shRNA reduction of CENP-U(50) in stable cell lines expressing LAP-CENP-U(50),

LAP-CENP-M, LAP-CENP-N, LAP-CENP-H, LAP-CENP-O and LAP-CENP-P. Cells were transfected with plasmid encoded shRNA against *CENP-U(50)* or control (pSUPER-hygro vector), in 10-fold molar excess to a gene expressing H2B-mRFP. Centromeres identified with ACA (red); LAP-CENP-U(50), LAP-CENP-H, LAP-CENP-O, LAP-CENP-M, LAP-CENP-N or LAP-CENP-P identified with antibodies to GFP (green). In all cases, cells with shRNA were identified by the presence of H2B-mRFP (data not shown). Exposure times for anti-GFP were constant within cell lines. The scale bars represent 5 μ m.

kinetochores, but without *CENP-U(50)*, Mad1 binding was significantly prolonged (Fig. 5g). Thus, *CENP-U(50)*-depleted kinetochores activated and sustained mitotic checkpoint signalling at individual kinetochores, but this was inefficiently silenced — indicative of a role for *CENP-U(50)* and its complexes in stable microtubule attachment. The cumulative effect of chromosomal missegregation due to lagging and misaligned chromosomes and delayed mitoses in cells that were chronically depleted of *CENP-U(50)* was severely reduced long-term viability, with colony formation reduced at least 150-fold compared with that of control cells.

CENP-A NAC is required for proper mitotic progression

siRNA depletion of the CENP-A NAC components *CENP-M*, *CENP-N* (alone or in combination) or *CENP-T* caused an increase in the number of cells in mitosis (Fig. 6a), with the reduction of *CENP-T* resulting in the greatest effect. This increase in mitotic index suggested that these cells are arrested or delayed in mitosis through the action of the mitotic checkpoint. Inspection of mitoses in cells with a reduced level of *CENP-M*, *CENP-N* or *CENP-T* revealed a similar spectrum of mitotic defects, again with reduction of *CENP-T* yielding the most pronounced phenotype (Fig. 6b).

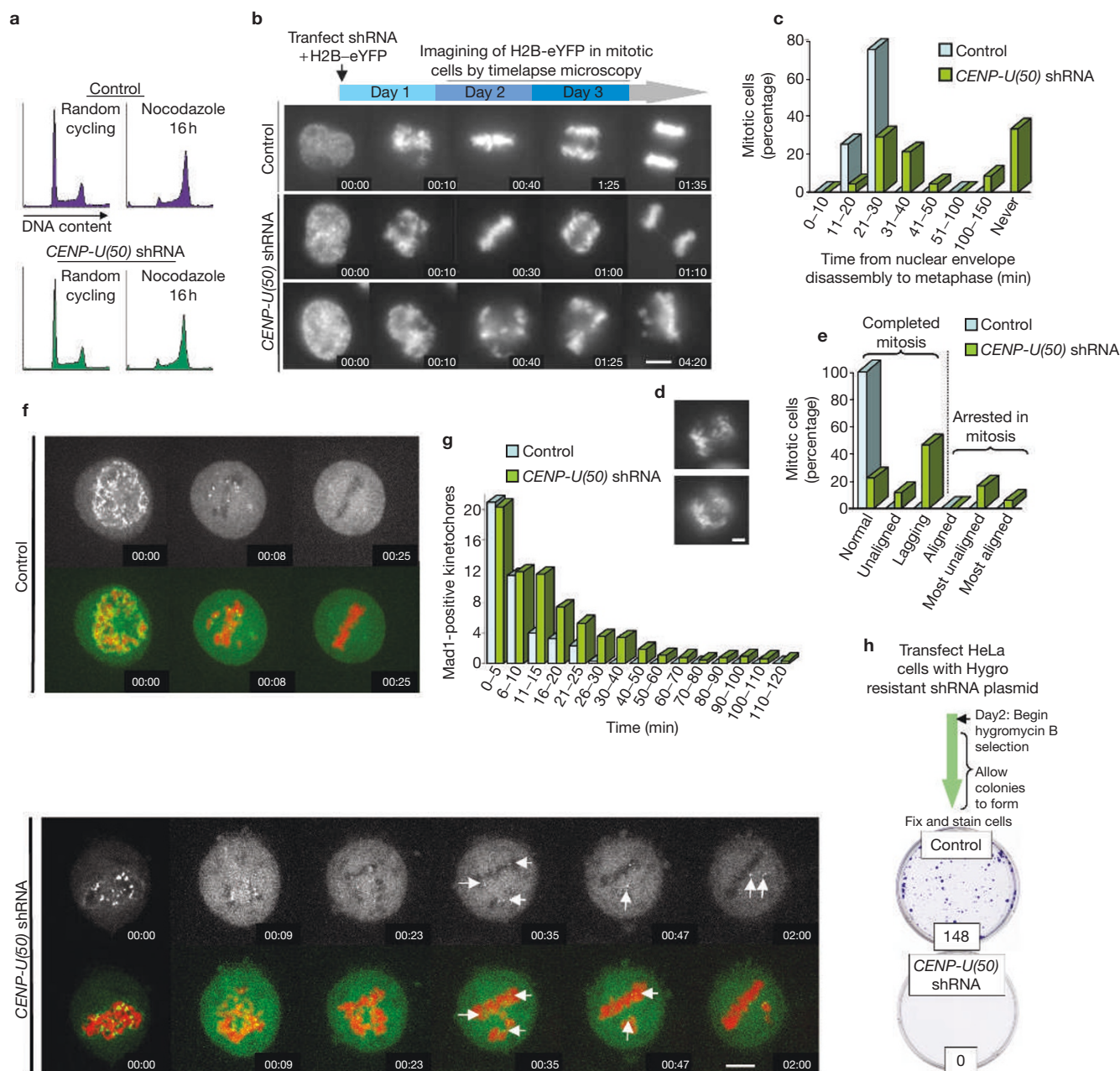


Figure 5 *CENP-U(50)* depletion causes mitotic errors without affecting the mitotic checkpoint. **(a)** FACS analysis of the GFP-positive population of cells after cotransfection of the *CENP-U(50)* shRNA plasmid or control plasmid and myristilated GFP gene (at a 10:1 ratio) and treatment with nocodazole for the final 16 h before harvesting at 72 h after transfection. **(b)** Live cell time-lapse microscopy was conducted on HeLa cells cotransfected with control (pSUPER-hygro) or *CENP-U(50)* shRNA plasmids at a 10:1 ratio with H2B-eYFP. Progression through mitosis was assayed 48–72 hours following transfection by time-lapse imaging of H2B-eYFP at 5 min intervals beginning at the initiation of chromosome condensation. The scale bar represents 5 μ m. **(c)** The time elapsed between nuclear envelope breakdown and the alignment of all chromosomes at metaphase in *CENP-U(50)* shRNA treated cells and control cells. **(d)** Examples of lagging chromosomes in *CENP-U(50)* knockdown cells. **(e)** Living cells assayed by time-lapse microscopy for mitotic

defects (*CENP-U(50)* shRNA, $n = 37$; control, $n = 10$). **(f)** Chromosome dynamics and YFP-Mad1 recruitment was followed by time-lapse microscopy in HeLa cells cotransfected with H2B-mRFP, eYFP-MAD1 and *CENP-U(50)* shRNA plasmid (at relative ratios of 1:1:10) using a spinning disc confocal microscope. **(g)** Average numbers of YFP-Mad1 positive kinetochores visible during the indicated time periods were assessed from live cell time-lapse images as in **f**. Two experiments were averaged for the experimental and control conditions. **(h)** Cell survival assayed by colony formation after transfecting HeLa cells with either a control plasmid (pSUPER-hygro; the parent vector to *CENP-U(50)* shRNA and which contains a hygromycin resistance gene) or a plasmid encoding shRNA directed against *CENP-U(50)*. After 14 days of selection with hygromycin B cells were fixed in methanol and stained with crystal violet. The number of individual colonies present after 14 days are given for each condition.

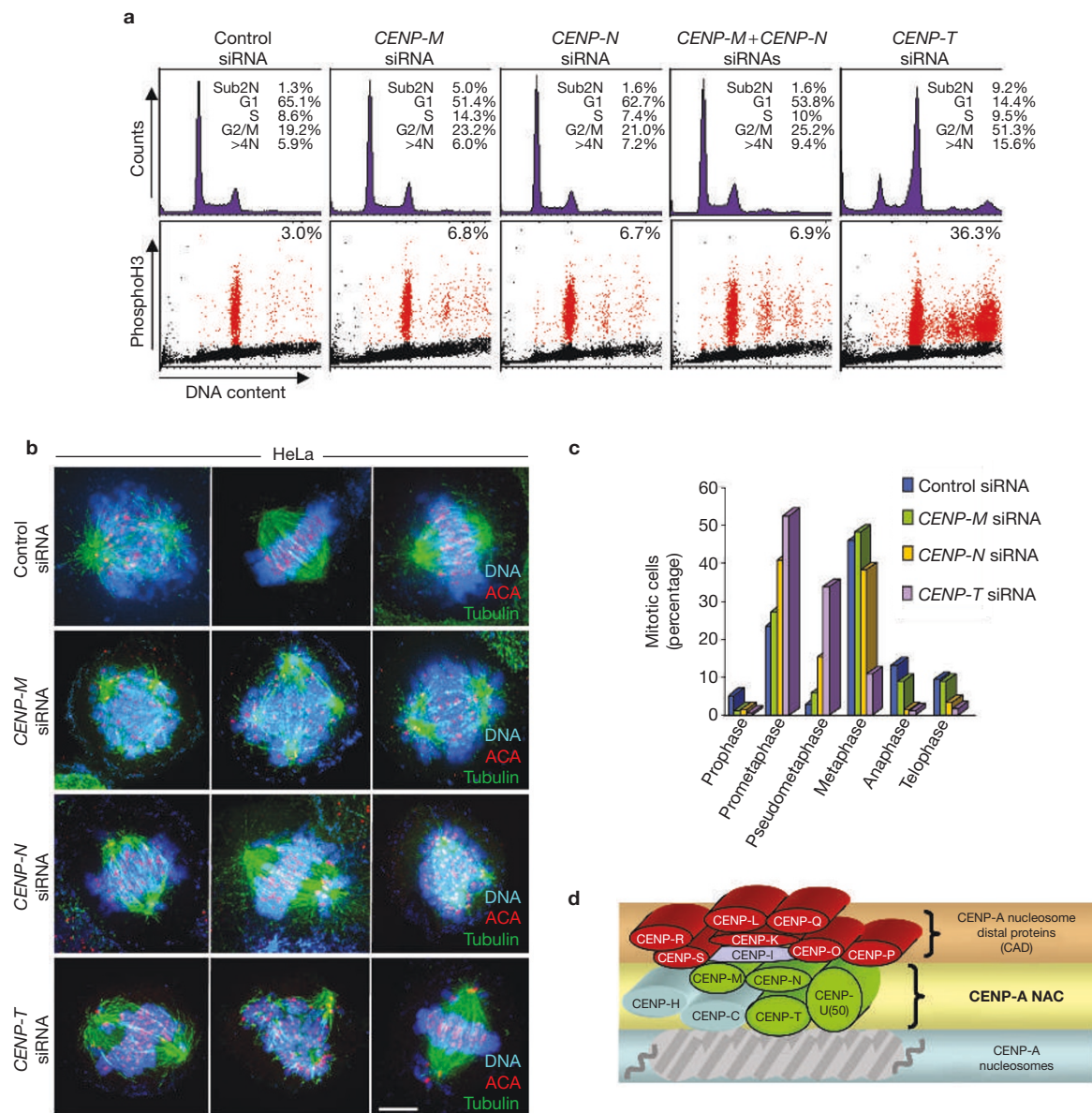


Figure 6 Mitotic defects due to CENP-A NAC disruption by depletion of *CENP-M*, *CENP-N* or *CENP-T*. **(a)** siRNA mediated reduction in *CENP-M*, *CENP-N* or *CENP-T* increases the proportion of cells in mitosis, as demonstrated by FACS analysis for DNA content and phosphohistone H3 staining. **(b)** Three examples of mitotic cells after introduction of a control siRNA or siRNAs against *CENP-M*, *CENP-N* or *CENP-T*.

These mitotic errors after disruption of the CENP-A NAC centered on a failure in chromosome congression (Fig. 6b, c) that yielded an increased proportion of cells in prometaphase or pseudometaphase (where one or more chromosomes are present at the spindle pole or along the spindle). Moreover, an increased number of cells with a greater than 4N DNA content was observed after reduction of *CENP-N* and *CENP-M* or *CENP-T* (Fig. 6a), indicating that at least a proportion of these cells eventually exit mitosis, but without cytokinesis. In each case, the phenotype of *CENP-T* siRNA treatment is more pronounced than that observed in *CENP-M* and *CENP-N* — possibly reflecting a unique role for CENP-T in centromere function. Taken together, although centromeres without the CENP-A NAC can recruit sufficient levels of mitotic checkpoint components to mount sustained checkpoint signalling when all chromosomes are

DNA stained with DAPI (blue); ACA (red) to mark centromeres; and tubulin (green). The scale bar represents 5 μ m. **(c)** Proportions of mitotic cells in each mitotic phase assessed in cells with reduced *CENP-M*, *CENP-N* or *CENP-T*. **(d)** The CENP-A NAC comprised of CENP-C, -H, -M, -N, -U(50) and -T directly mediates the interaction between the CENP-A nucleosome and the CAD centromere.

unattached to spindle microtubules, they are unable to make or sustain stable microtubule capture which produces chromosome misalignment before the onset of anaphase and fatal chromosome missegregation in the subsequent steps of mitosis.

DISCUSSION

The complex array of DNA repeats found in human centromeres has long suggested a subunit model for the assembly of mammalian centromeres⁴⁵. Although these repetitive arrays could, in principle, recruit components only in the context of this complex centromeric chromatin, our evidence makes it clear that the CENP-A NAC (comprised of the newly identified CENP-M, CENP-N, and CENP-T, and the previously identified CENP-U(50), CENP-C, and CENP-H) recognizes and remains

stably bound to one (or at most a handful) of CENP-A-containing nucleosomes. Depletion of *CENP-M*, *CENP-N* and *CENP-T* results in the loss of each other and of CENP-H. CENP-H, in turn, is required for centromere association of CENP-C¹⁶. Thus, the ability of the CENP-A NAC to recognize CENP-A nucleosomes is dependent on CENP-M, CENP-N and CENP-T, strongly implicating an activity of one or more of these, either alone or in the context of the complete CENP-A NAC, in distinguishing CENP-A nucleosomes from those assembled with histone H3.

Given that the assembly of subnucleosomal heterotetramers of histone H4 with CENP-A produces heterotetramers that are structurally more rigid than those containing histone H3 (ref. 7), our evidence demonstrates that even at the level of one (or a few) nucleosomes, a sufficiently unique environment is produced by assembly of CENP-A into chromatin to stably associate with the CENP-A NAC. The presence of this complex then recruits seven more distal CAD components that do not recognize CENP-A nucleosomes directly. Considered with the observation that localization of CENP-I is dependent on CENP-H¹⁶, it seems that centromeric association of many (if not all) of the CAD components are dependent on the CENP-A NAC.

Disruption of the CENP-A NAC by reduction of CENP-M, CENP-N or CENP-T results in the loss from kinetochores of multiple CENP-A NAC components and a pronounced mitotic defect, where cells are unable to properly align their chromosomes and generates a significant mitotic delay. These phenotypes are similar to those observed with the deletion of CENP-I or CENP-H in chicken cells, each of which leads to chromosome missegregation and prolonged mitotic arrest^{16,17}. Removal of CENP-U(50) also leads to errors in microtubule attachment and chromosome alignment³² (Fig. 5), albeit to a lesser degree. In each case, the CENP-A NAC and its associated CAD proteins are essential for stabilizing microtubule attachment but not for components of mitotic checkpoint signalling, whose recruitment to CENP-A nucleosomes is independent of the CENP-A NAC.

The role of the known CAF-1 proteins in centromere assembly remains unclear. In the mammalian context, the CAF-1 complex and HIRA (the human homologue of the *S. cerevisiae* histone regulatory Hir proteins) are independently responsible for loading histone H3.1 and H3.3, respectively²⁸. Depletion of the human CAF-1 complex members, RbAp46 and RbAp48, or a fission yeast counterpart Mis16, results in the loss of CENP-A from centromeres⁴⁶. However, the CAF-1 and HIRA complexes are absent from CENP-A nucleosomes preparations, raising the question of which factors, if any, are responsible for CENP-A nucleosome assembly. We cannot exclude the possibility that, unlike the most abundant histone H3 variant (H3.1) that is loaded during S phase, the CAF-1 complex (or another chromatin loader) may associate only with the prenucleosomal complex(es) of CENP-A. However, our evidence strongly implies that loading of CENP-A occurs through a mechanism distinct from the CAF-1 and HIRA factors.

We have also determined that centromeric CENP-A-containing nucleosomes are more likely than their H3.1 counterparts to contain the histone H2A variants macroH2A and H2A.Z. Given the previously established role of the FACT complex (which is shown here to interact with the CENP-A nucleosome) in sequestering H2A:H2B during RNA polymerase II mediated transcription⁴⁷, the FACT complex may mediate H2A:H2B interactions with the CENP-A nucleosome, possibly facilitating the exchange of canonical H2A:H2B dimers for those containing the H2A.Z or macroH2A variants within the centromere. Incorporation of

different H2A variants, as well as assembly of a subset of heterotypic CENP-A:H3 nucleosomes (Fig. 1e) or the posttranslational modification of either CENP-A or the other histones, may allow for multiple permutations of the CENP-A nucleosome, ultimately suggesting that the centromeric nucleosome may be more complex than previously thought. □

Note added in proof: an accompanying manuscript by Okada, M. et al. (Nature Cell Biol. 8, 446–457; 2006) is also published in this issue

METHODS

Plasmids. The open reading frames (ORFs) of CENP-A (NM_001809), Histone H3.1 (NM_003537), CENP-M (NM_024053), CENP-N (NM_018455), CENP-T (AAH15202), CENP-U(50) (NM_024629), CENP-R (NM_014288) and CENP-S (NM_199294) were obtained by PCR amplification. CENP-A and histone H3.1 TAP constructs were cloned into a vector containing the S-protein-TEV-protein-A TAP tag resulting in fusion of the tag to the 3' end of the ORF. LAP tagged constructs of CENP-M, CENP-N, CENP-T, CENP-U(50), CENP-R and CENP-S were constructed in the pC113 vector containing the LAP tag at the amino (N)terminus³⁴. ORFs containing the TAP and LAP tagged constructs were then subcloned into the *Sna*B1 and *Eco*RI sites of the retroviral pBABE-Puro vector. Short hairpin (sh) RNA was expressed from a modified pSUPER vector containing a hygromycin resistance cassette. shRNA against CENP-U(50) (also known as MLF1IP) was constructed as previously described⁴⁴ from two complimentary oligonucleotides that contained base pairs 127–145 of the CENP-U(50) ORF.

Stable cell lines and siRNA treatment. TAP and LAP constructs in the pBABE-Puro vector were cotransfected with a plasmid expressing VSV-G into the 293GP packaging cell line to produce pseudotyped amphotropic retrovirus as previously described⁴⁴. HeLa cells were infected with retrovirus by incubating with supernatant derived from pBABE-Puro transfected 293GP cells and selected for 2 weeks in 1.5 μ g ml⁻¹ puromycin after which single-cell clones were isolated. In the case of LAP tagged constructs, clones were isolated using fluorescence activated cell sorting (FACS Vantage; Becton Dickinson, Franklin Lakes, NJ). Cell lines expressing LAP-CENP-H, LAP-CENP-O and LAP-CENP-P were generously provided by I. Cheeseman (LICR, San Diego, CA). HeLa and stable cell lines were maintained in DMEM with 10% newborn calf serum.

Plasmid based shRNAs used to repress CENP-U(50) and CENP-A were transfected into HeLa cells and established cell lines together with H2B-mRFP as a marker of transfection at a ratio 10:1 using Effectene (Qiagen, Valencia, CA). Cells were examined by immunocytochemistry or live-cell microscopy 48–72 h (CENP-U(50)) or 120 h (CENP-A) following initiation of transfection. siRNAs were introduced into HeLa cells and established cell lines using Oligofectin (Invitrogen, Carlsbad, CA). Cells were plated at a density of 1.3×10^5 per 3-cm dish and treated with duplex siRNA oligonucleotides at a concentration of 100 nM. siRNAs against CENP-M, CENP-N and CENP-T were purchased from Dharmacon (Lafayette, CO) as presynthesized pools of four unique siRNAs directed against each mRNA. siRNAs directed against GAPDH were used as a control for all siRNA experiments.

Affinity purification. Three independent stable cell lines were used for each affinity purification experiment. Nuclei from 1×10^9 HeLa cells were prepared similar to previous methods⁴⁸, by pelleting and resuspending cells in buffer containing 3.75 mM Tris at pH 7.5, 20 mM KCl, 0.5 mM EDTA, 0.5 mM DTT, 0.05 mM spermidine, 0.125 mM spermine, 1 mM PMSF and 0.1% digitonin. Cells were homogenized with 10 strokes and nuclei were pelleted at 300g. Nuclei were then washed once in wash buffer (20 mM HEPES at pH 7.7, 20 mM KCl, 0.5 mM EDTA, 0.5 mM DTT and 0.5 mM PMSF), followed by wash buffer containing 300 mM NaCl. Nuclei were resuspended in wash buffer supplemented with 300 mM NaCl and 3 mM CaCl₂. Chromatin was digested for 1 h at room temperature using 140 units ml⁻¹ of micrococcal nuclease (cat# 10107921001; Roche, Indianapolis, IN). Following micrococcal nuclease treatment, extracts were supplemented with 5 mM EGTA and 0.05% NP40 and centrifuged at 10,000g for 15 min at 4 °C. The supernatant was then used as the starting material for all tandem affinity purifications. Tandem affinity purification for the proteins containing the TAP tag were conducted by first purifying complexes from the soluble nucleosome fraction using random rabbit IgG bound to Ultralink (Pierce, Rockford, IL). Alternatively, LAP tags were first purified using anti-GFP antibody

coupled to Affiprep Protein-A (Biorad, Hercules, CA)³⁴. Chromatin extracts were incubated with antibody bound beads for 2 h at 4 °C. Bound complexes were washed once in buffer A (20 mM HEPES at pH 7.7, 20 mM KCl, 0.4 mM EDTA and 0.4 mM DTT), once in buffer A with 300 mM KCl and finally in buffer A with 300 mM KCl, 1 mM DTT and 0.1% Tween 20. Complexes were incubated 16 h in final wash buffer with 50 µl recombinant TEV protease. Complexes were then further purified by binding to S-protein agarose (Novagen, San Diego, CA) and incubating for 3 h at 4 °C. Complexes were washed in buffer B (20 mM HEPES at pH 7.7, 0.5 mM EDTA, 0.5 mM DTT) with 300 mM KCl, followed by 100 mM KCl and eluted with 8 M urea in 50 mM Tris at pH 8.5.

Mass spectrometry. Eluates were reduced and digested in solution using trypsin (0.5 µg µl⁻¹ in 1% acetic acid; Roche). Digested samples were then loaded onto a three phase MudPIT column consisting of 8–9 cm Aqua 3u C18 125A resin (Phenomenex, Torrance, CA), 2–3 cm Luna 5u strong cation exchange 100A resin (Phenomenex) and 3–4 cm Aqua 5u C18 resin (Phenomenex). Six chromatography steps were performed and analysed in-line using a Finnigan LCQ Deca ion-trap mass spectrometer⁴⁹. Spectra were collected in a data-dependent manner by taking a single mass spectrometry (MS) scan followed by MS–MS scans of the top three most intense ions. Qualifying spectra were searched against a current NCBI *Homo sapiens* concatenated database using the SEQUEST algorithm and further filtered using DTASelect using XCorr cutoff values of 1.5, 2.0, 2.5 and 3.0 for +1, +2, +3 and +4 charged peptides respectively. (DeltCN cutoff value of 0.05 and required a minimum of 2 peptides per protein).

Immunocytochemistry Cells were preextracted in PBS using 0.3% Triton X-100 for 3 min followed by 20 min fixation in 4% formaldehyde. Cell were blocked in 2.5% FBS, 2 M glycine, 0.1% Triton X-100 in PBS for 1 h. Antibody incubations were conducted in the blocking solution for 1 h. DNA was detected using DAPI and cells were mounted in Prolong Antifade (Invitrogen). Centromeres were detected using ACA sera (1:500; Antibodies Inc., Davis, CA), anti-CENP-B (mAb 2D7, 1:100)³⁵ and microtubules using DM1A monoclonal antibodies (1:5000). For fixed cells, LAP tags were detected using a rabbit anti-GFP antibody (1:1000). TAP tags were detected using FITC conjugated rabbit IgG. CENP-A was detected in fixed cells without pre-extraction using monoclonal anti-CENP-A antibodies. Images were collected on a Deltavision deconvolution microscope (Applied Precision, Issaquah, WA). z-stack projections were assembled for each image.

Flow cytometry. siRNA treated cells were harvested in PBS with 3 mM EGTA, washed in PBS and fixed in 70% ethanol. Cells were stained for phosphorylated histone H3 by blocking cells in PBS with 0.1% BSA and 0.5% Tween 20 and then incubating cells with anti-phosphoH3 antibody (1:300; Cat #06-755; Upstate Biotech, Charlottesville, VA), cells were then washed and incubated with FITC conjugated secondary antibody. DNA was stained by incubating cells for 30 min with 1% FBS, 10 µg ml⁻¹ propidium iodide and 0.25 mg ml⁻¹ RNase A in PBS followed by FACS analysis using a Becton Dickinson FACSsort.

Live-cell microscopy. Cells were plated on glass-bottomed 3-cm tissue culture plates (Mattek Inc., Ashland, MA) and cotransfected with either eYFP–H2B or eYFP–Mad1 and pSUPER–hygro plasmid at a ratio of 1:10 using Effectene (Qiagen). After 48–72 h, cells were transferred to CO₂ independent media (Invitrogen) supplemented with 10% newborn calf serum, 100 units ml⁻¹ penicillin, 100 units ml⁻¹ streptomycin and 2 mM L-glutamine. H2B–eYFP expressing cells were imaged on a Nikon Eclipse TE300 using a ×100 objective and Coolsnap HQ (Photometrics, Tucson, AZ) CCD camera using and Metamorph software. Cells expressing eYFP–Mad1 were imaged using a spinning disk confocal (McBain Instruments, Chatsworth, CA) connected to a Nikon TE200e inverted microscope. Images were collected using a ×60 1.4 NA objective lens. z-stacks (5 planes, 1 µm each) were acquired at 2 min intervals using a Hamamatsu Orca ER camera and Metamorph software.

Colony formation assays. HeLa cells were transfected with pSUPER–hygro or pSUPER–hygro containing *CENP-U(50)* shRNA using Effectene (Qiagen). The following day, cells were supplemented with 0.4 µg ml⁻¹ hygromycin B and the media was replaced every two days thereafter. After 14 days in culture, cells were fixed in 100% methanol and stained with 0.2% crystal violet for 30 min and washed in PBS.

RNA quantification. In the case of CENP-U(50), cells were transfected with pBABE–Puro (empty vector) and either pSUPER–hygro or pSUPER–hygro containing the *CENP-U(50)* shRNA at a ratio of 1:10. After 24 h, cells were treated with 1.5 µg ml⁻¹ puromycin for 48 h, at which time cells were harvested. For all siRNA treated conditions, cells were seeded on 3-cm plates and treated with siRNA oligonucleotides as described above. Cells were harvested 72 h after initiation of siRNA treatment. RNA was isolated using Trizol (Invitrogen) and cDNA was synthesized from 1 µg (CENP-U(50)) or 3 µg total RNA using Superscript II Reverse Transcriptase (Invitrogen). Quantitative PCR from cDNA was conducted using Biorad iQ SYBR green supermix in an iCycler (Biorad). Threshold cycle counts were normalized to GAPDH levels in each treatment condition and used to calculate the percent reduction compared with control shRNA or luciferase siRNA treated controls.

Note: Supplementary Information is available on the Nature Cell Biology website.

ACKNOWLEDGEMENTS

The authors thank T. Fukagawa, I. Cheeseman, J. Shah, P. Maddox, K. Weis, F. Furnari and K. Yoda for generously providing reagents and assistance; D. Young and the University of California at San Diego (UCSD) Cancer Center for flow cytometry and the Oegema and Desai laboratories for use of spinning disk confocal and deconvolution microscopes. This work has been supported by grants from the National Institutes of Health (NIH) to D.W.C. (GM 29513) and J.R.Y. (RR11823). D.R.F. has been supported by a postdoctoral fellowship from the NIH and B.E.B. has been supported by a postdoctoral fellowship from the American Cancer Society and in part by a Career Award in the Biomedical Sciences from the Burroughs Wellcome Fund. D.W.C. receives salary support from the Ludwig Institute for Cancer Research.

COMPETING FINANCIAL INTERESTS

The authors declare that they have no competing financial interests.

Published online at <http://www.nature.com/naturecellbiology/>

Reprints and permissions information is available online at <http://npg.nature.com/reprintsandpermissions/>

- Cleveland, D. W., Mao, Y. & Sullivan, K. F. Centromeres and kinetochores: from epigenetics to mitotic checkpoint signaling. *Cell* **112**, 407–421 (2003).
- Amor, D. J., Kalitsis, P., Sumer, H. & Choo, K. H. Building the centromere: from foundation proteins to 3D organization. *Trends Cell Biol.* **14**, 359–368 (2004).
- Amor, D. J. & Choo, K. H. Neocentromeres: role in human disease, evolution, and centromere study. *Am. J. Hum. Genet.* **71**, 695–714 (2002).
- Henikoff, S. & Ahmad, K. Assembly of variant histones into chromatin. *Annu. Rev. Cell Dev. Biol.* **21**, 133–153 (2005).
- Sullivan, B. A., Blower, M. D. & Karpen, G. H. Determining centromere identity: cyclical stories and forking paths. *Nature Rev. Genet.* **2**, 584–596 (2001).
- Blower, M. D., Sullivan, B. A. & Karpen, G. H. Conserved organization of centromeric chromatin in flies and humans. *Dev. Cell* **2**, 319–330 (2002).
- Black, B. E. *et al.* Structural determinants for generating centromeric chromatin. *Nature* **430**, 578–82 (2004).
- Cheeseman, I. M., Drubin, D. G. & Barnes, G. Simple centromere, complex kinetochore: linking spindle microtubules and centromeric DNA in budding yeast. *J. Cell Biol.* **157**, 199–203 (2002).
- McAinsh, A. D., Tytell, J. D. & Sorger, P. K. Structure, function and regulation of budding yeast kinetochores. *Annu. Rev. Cell Dev. Biol.* **19**, 519–539 (2003).
- Howman, E. V. *et al.* Early disruption of centromeric chromatin organization in centromere protein A (*Cenpa*) null mice. *Proc. Natl Acad. Sci. USA* **97**, 1148–1153 (2000).
- Fukagawa, T., Pendon, C., Morris, J. & Brown, W. CENP-C is necessary but not sufficient to induce formation of a functional centromere. *EMBO J.* **18**, 4196–4209 (1999).
- Meluh, P. B. & Koshland, D. Evidence that the *MIF2* gene of *Saccharomyces cerevisiae* encodes a centromere protein with homology to the mammalian centromere protein CENP-C. *Mol. Biol. Cell* **6**, 793–807 (1995).
- Goshima, G., Kiyomitsu, T., Yoda, K. & Yanagida, M. Human centromere chromatin protein hMis12, essential for equal segregation, is independent of CENP-A loading pathway. *J. Cell Biol.* **160**, 25–39 (2003).
- Goshima, G., Saitoh, S. & Yanagida, M. Proper metaphase spindle length is determined by centromere proteins Mis12 and Mis6 required for faithful chromosome segregation. *Genes Dev.* **13**, 1664–1677 (1999).
- Liu, S. T. *et al.* Human CENP-I specifies localization of CENP-F, MAD1 and MAD2 to kinetochores and is essential for mitosis. *Nature Cell Biol.* **5**, 341–345 (2003).
- Nishihashi, A. *et al.* CENP-I is essential for centromere function in vertebrate cells. *Dev. Cell* **2**, 463–476 (2002).
- Fukagawa, T. *et al.* CENP-H, a constitutive centromere component, is required for centromere targeting of CENP-C in vertebrate cells. *EMBO J.* **20**, 4603–4617 (2001).
- Bomont, P., Maddox, P., Shah, J. V., Desai, A. B. & Cleveland, D. W. Unstable microtubule capture at kinetochores depleted of the centromere-associated protein CENP-F. *EMBO J.* **24**, 3927–3939 (2005).
- Mao, Y., Desai, A. & Cleveland, D. W. Microtubule capture by CENP-E silences BubR1-dependent mitotic checkpoint signaling. *J. Cell Biol.* **170**, 873–880 (2005).

20. Obuse, C. *et al.* Proteomics analysis of the centromere complex from HeLa interphase cells: UV-damaged DNA binding protein 1 (DDB-1) is a component of the CEN-complex, while BMI-1 is transiently co-localized with the centromeric region in interphase. *Genes Cells* **9**, 105–120 (2004).
21. Cheeseman, I. M. *et al.* Implication of a novel multiprotein Dam1p complex in outer kinetochore function. *J. Cell Biol.* **155**, 1137–1145 (2001).
22. Smith, S. & Stillman, B. Stepwise assembly of chromatin during DNA replication *in vitro*. *EMBO J.* **10**, 971–980 (1991).
23. Jackson, V. *In vivo* studies on the dynamics of histone–DNA interaction: evidence for nucleosome dissolution during replication and transcription and a low level of dissolution independent of both. *Biochemistry* **29**, 719–731 (1990).
24. Shelby, R. D., Vafa, O. & Sullivan, K. F. Assembly of CENP-A into centromeric chromatin requires a cooperative array of nucleosomal DNA contact sites. *J. Cell Biol.* **136**, 501–513 (1997).
25. Eickbush, T. H. & Moudrianakis, E. N. The histone core complex: an octamer assembled by two sets of protein–protein interactions. *Biochemistry* **17**, 4955–4964 (1978).
26. Masumoto, H., Masukata, H., Muro, Y., Nozaki, N. & Okazaki, T. A human centromere antigen (CENP-B) interacts with a short specific sequence in alphoid DNA, a human centromeric satellite. *J. Cell Biol.* **109**, 1963–1973 (1989).
27. Verreault, A., Kaufman, P. D., Kobayashi, R. & Stillman, B. Nucleosome assembly by a complex of CAF-1 and acetylated histones H3/H4. *Cell* **87**, 95–104 (1996).
28. Tagami, H., Ray-Gallet, D., Almouzni, G. & Nakatani, Y. Histone H3.1 and H3.3 complexes mediate nucleosome assembly pathways dependent or independent of DNA synthesis. *Cell* **116**, 51–61 (2004).
29. Maison, C. & Almouzni, G. HP1 and the dynamics of heterochromatin maintenance. *Nature Rev. Mol. Cell Biol.* **5**, 296–304 (2004).
30. Sarma, K. & Reinberg, D. Histone variants meet their match. *Nature Rev. Mol. Cell Biol.* **6**, 139–149 (2005).
31. Hanissian, S. H. *et al.* cDNA cloning and characterization of a novel gene encoding the MLF1-interacting protein MLF1IP. *Oncogene* **23**, 3700–3707 (2004).
32. Minoshima, Y. *et al.* The constitutive centromere component CENP-50 is required for recovery from spindle damage. *Mol. Cell Biol.* **25**, 10315–10328 (2005).
33. Bierie, B., Edwin, M., Joseph Melenhorst, J. & Hennighausen, L. The proliferation associated nuclear element (PANE1) is conserved between mammals and fish and preferentially expressed in activated lymphoid cells. *Gene Expr. Patterns* **4**, 389–395 (2004).
34. Cheeseman, I. M. & Desai, A. A combined approach for the localization and tandem affinity purification of protein complexes from metazoans. *Sci. STKE* DOI:10.1126/stke.2662005p11 (2005).
35. Earnshaw, W. C. *et al.* Molecular cloning of cDNA for CENP-B, the major human centromere autoantigen. *J. Cell Biol.* **104**, 817–829 (1987).
36. Saitoh, H. *et al.* CENP-C, an autoantigen in scleroderma, is a component of the human inner kinetochore plate. *Cell* **70**, 115–125 (1992).
37. Sugata, N., Munekata, E. & Todokoro, K. Characterization of a novel kinetochore protein, CENP-H. *J. Biol. Chem.* **274**, 27343–27346 (1999).
38. Orphanides, G., Wu, W. H., Lane, W. S., Hampsey, M. & Reinberg, D. The chromatin-specific transcription elongation factor FACT comprises human SPT16 and SSRP1 proteins. *Nature* **400**, 284–288 (1999).
39. Okuwaki, M., Matsumoto, K., Tsujimoto, M. & Nagata, K. Function of nucleophosmin/B23, a nucleolar acidic protein, as a histone chaperone. *FEBS Lett.* **506**, 272–276 (2001).
40. Okuda, M. The role of nucleophosmin in centrosome duplication. *Oncogene* **21**, 6170–6174 (2002).
41. Brummelkamp, T. R., Bernards, R. & Agami, R. A system for stable expression of short interfering RNAs in mammalian cells. *Science* **296**, 550–553 (2002).
42. Regnier, V. *et al.* CENP-A is required for accurate chromosome segregation and sustained kinetochore association of BubR1. *Mol. Cell Biol.* **25**, 3967–3981 (2005).
43. Chen, R. H., Shevchenko, A., Mann, M. & Murray, A. W. Spindle checkpoint protein Xmad1 recruits Xmad2 to unattached kinetochores. *J. Cell Biol.* **143**, 283–295 (1998).
44. Shah, J. V. *et al.* Dynamics of centromere and kinetochore proteins; implications for checkpoint signaling and silencing. *Curr. Biol.* **14**, 942–952 (2004).
45. Zinkowski, R. P., Meyne, J. & Brinkley, B. R. The centromere–kinetochore complex: a repeat subunit model. *J. Cell Biol.* **113**, 1091–1110 (1991).
46. Hayashi, T. *et al.* Mis16 and Mis18 are required for CENP-A loading and histone deacetylation at centromeres. *Cell* **118**, 715–729 (2004).
47. Belotserkovskaya, R. *et al.* FACT facilitates transcription-dependent nucleosome alteration. *Science* **301**, 1090–1093 (2003).
48. Yoda, K., Morishita, S. & Hashimoto, K. Histone variant CENP-A purification, nucleosome reconstitution. *Methods Enzymol.* **375**, 253–269 (2004).
49. MacCoss, M. J. *et al.* Shotgun identification of protein modifications from protein complexes and lens tissue. *Proc. Natl Acad. Sci. USA* **99**, 7900–7905 (2002).

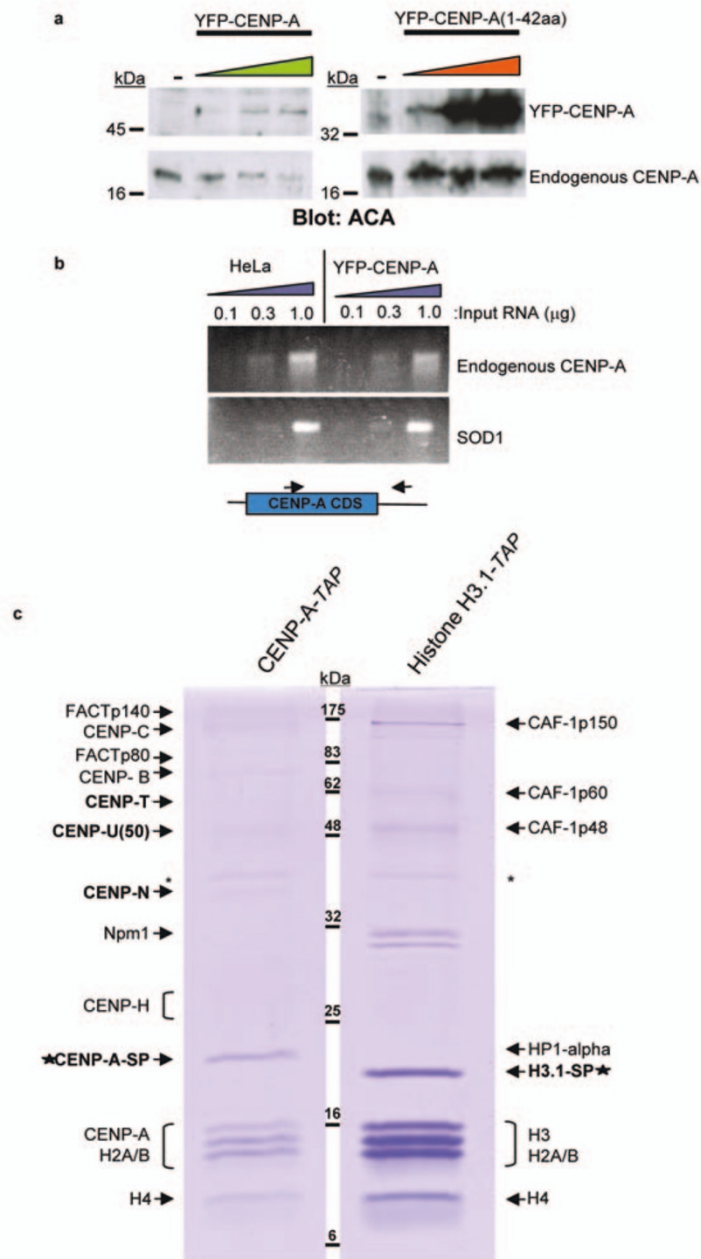


Figure S1 (a) Stable cell populations expressing varying amounts of full-length YFP-CENP-A or amino acids 1-42 of CENP-A (YFP-CENP-A(1-42)) were established and extracts were immunoblotted with an ACA serum to assess the levels of endogenous and tagged CENP-A. (b) Amounts of endogenous and YFP-tagged CENP-A mRNAs were determined using RT-PCR of RNA derived from HeLa cells and cells from a) with the highest

accumulated of YFP-CENP-A. For the endogenous CENP-A mRNA, a primer from the 3' untranslated region was used to avoid amplification of the exogenous YFP-CENP-A mRNA (which contained only the CENP-A open reading frame). (c) The doubly affinity purified preparations of CENP-A and histone H3.1 containing nucleosomes shown in Fig. 1 analyzed here by 12% SDS-PAGE and visualization with Coomassie blue staining.

a

```

1  -----MSVLRPLDK-----LPGLNTATILLVG--TEDALLQQL--ADSMKEDC-----
1  -----MSVLRSMDEK-----LPDLNRRATVLLVS--TEDALLQQL--AESMLKDDC-----
1  -----MATLRFFDK-----MPMLNAAALLLVG--TEESHREQL--ASAMLKPEK-----
1  MVSQVLSHQRFLSKRALTCHVQLSHMETPQLQLNSRYEYSCYVPLGISQAYLHTDCPAPC

41  -----ASELKVHLAKSLPLPSSVN--RPRIDLIVFVVNLHLSKYSLQNTES
41  -----ASELRVHLANSPLPSSNVN--RPRIDLIVFVINLHLSKYSLOKVEEF
41  -----TFEVKIHMAQSLPLFYEREHLRPRFDMVVFILNLSQFSLSTVLAS
61  PQDRLQAGIPVRGPAARAAQHHLASSLPLPSERDHLRPRIDLIAFVIDIKSKYSLKNVQAS

85  LRHVDAFFLGKVCFLATGAGRESHCSIHRTTVVKLAHTYQSPFLLYCDLEVEGFRATMAQ
85  LQHVDSFFLGKVCFLVTGAGQESHCSVHQNTVIKLAHTYRSPLLLCDLQVESFRAAMAR
87  LTHLDVNFLLGKVCFAITGGGVKHKCMVDIATVKKLADTHLSTLLFSEFDSDDVTCTAR
121  LAYVDVRFLLGKVCFLVTGVGRANNCSEVMNAIWKLGEDYCSFVIFCELELEGIRVATAQ

145  RLVRVLQICAGHVPGVSAALNLLSLRSSEGPSLEDL
145  RLVRILQICAGHVPGVSAALNLLSLRSPENPFPSKEL
147  RLQMVQICAGLVPGISALYLGSFMNST--LQTDQF
181  RLLRMQLICAGRVPGVSALYFSLMNRNS---AGD

```

H. Sapiens CENP-M NP_076958
M. musculus CENP-M XP_487040
X. leavis CENP-M NP_001017175
G. Gallus CENP-M XP_416221-1

H. Sapiens CENP-M NP_076958
M. musculus CENP-M XP_487040
X. leavis CENP-M NP_001017175
G. Gallus CENP-M XP_416221-1

H. Sapiens CENP-M NP_076958
M. musculus CENP-M XP_487040
X. leavis CENP-M NP_001017175
G. Gallus CENP-M XP_416221-1

H. Sapiens CENP-M NP_076958
M. musculus CENP-M XP_487040
X. leavis CENP-M NP_001017175
G. Gallus CENP-M XP_416221-1

b

```

1  MDETVAEF-----IKRTILKIPMNELTTLKAWDFLSENQLQTVNFR
1  MKENVAEF-----LRRTILKIPLEMKSILEAWDFLSEDLQQTINLK
1  MAPAAEIVQKKRQSSALVMDIEWIAEFIKRTILKLPFSQTMITLKAQGLTDSLQTLTLR
1  MDEQARSV-----LNRVIRRIIPNKNIKNLKSKWNCLSDQLQALDYT

43  QRKESVVQHLIHLCEEKRASISDAALLDIYMQFHQKQVWDFVQMSKFGF--EDVDLFDM
43  QRKDYLAQEVILLCEDEKRAALDDVVLDDIVYTQFHRHQKLWNVFQMSKEFG--EDVDLFDM
61  YPKDITATEVVRLECAKNAITIDHAAALDVFNFHAFSNKKLWTVYQMSKTSE--SENDLFDA
43  KPKRMIVHEHITDCESSSLNLKHITNLEMIIYHLDNDQGTWYACQLTDAQD--DAVCV-EL

102  KQFKNSFKKILQRALKNVTVSFRETEENAVWIRIAWGTQYTKPNQYKPTYVYVYSQTPYA
102  EQFQSSFKRILQRALKNVTVSFRVYVYKDSVWIRVWAGTQYSPNQYKPTFVYVYVYQTPYA
120  SEFKLQFKKSIHAVSKNVTINFKEF--GEALWIRIAWGTHTNTRPNQYKATFAVYHSTPHV
101  TQFKEQFKAHLSHGVIRHISIKMKKHEDDAIWIIRIAGWDFNSKFNHLKPTYVYVHHLHTSYV

162  FTSSMLRRNTFLLGQALTIASKHHQIVKMDLRSRYLDSLKAIVFKQYNQTFETHNSTTF
162  FISSCHLKNTVPLHLQALKVASKHHQIVHLDLRSRHLDSLKAIVFREYNQTCENYSSTTS
179  FIT-GLGKACRPLLCQALVIAASKYSQIQEMELKSRCLSESLKDIFVKRFNQPFSSHHSR--
161  FIS-NLMAKKHIFLCQALVVAATRIGSLIKDGHLLSTRSLTAMRDLLRLRYQQVFPSAQSK--

222  LQER---SLGLDINMDSRIIHENIVEKERVQRITQETFGDYPPQPLEFAQYKLETKFKS
222  LQEA---SLSM--CLDSKIITHENTEEKVRVHRVTQETFGTYPPQPLEFAQYKLETKFKS
236  PHEK---ALTQKI-VDPFRVTYENMREKERVHHLTRETFGEGPLPKLELASYKLETMFRA
218  IQQERDSPPHPCI-GKEHSDYEEMR-----HQMACEAFGHGPTPKLETAQYKLETRYRG

278  GLNGSI--LAEREEPLRCLIKFSSPHLLEALKSLAPAGIADAPLSPLLTICIPNKRMYFK
276  NIGGGL--LADNKEPFRCVLKFSPPHLEALKSLAPAGIADAPLSPLLTICIPSKKMYFK
291  E-SIMGGNLTAGNEPFRVCVVKFSSPHLLEAIRSLAPAGIAEAPISTLLSCIPHKARNSEFK
272  N-GNLT--VSDREEFFRGGVVRFSSSSLLSRLNCVASGMAEGFVTPLLSAITRRGRNSFV

336  IRDK-----
334  IRDK-----
350  ITEK-RGLHPASSQPTNF
329  ITDKGGPGVSSQASAPRA

```

H. Sapiens CENP-N NP_060925
M. musculus CENP-N NP_082407
X. leavis CENP-N NP_001011097
D. Rerio CENP-N AAT68149

H. Sapiens CENP-N NP_060925
M. musculus CENP-N NP_082407
X. leavis CENP-N NP_001011097
D. Rerio CENP-N AAT68149

H. Sapiens CENP-N NP_060925
M. musculus CENP-N NP_082407
X. leavis CENP-N NP_001011097
D. Rerio CENP-N AAT68149

H. Sapiens CENP-N NP_060925
M. musculus CENP-N NP_082407
X. leavis CENP-N NP_001011097
D. Rerio CENP-N AAT68149

H. Sapiens CENP-N NP_060925
M. musculus CENP-N NP_082407
X. leavis CENP-N NP_001011097
D. Rerio CENP-N AAT68149

H. Sapiens CENP-N NP_060925
M. musculus CENP-N NP_082407
X. leavis CENP-N NP_001011097
D. Rerio CENP-N AAT68149

H. Sapiens CENP-N NP_060925
M. musculus CENP-N NP_082407
X. leavis CENP-N NP_001011097
D. Rerio CENP-N AAT68149

Figure S2 Identification of CENP-M and CENP-N vertebrate homologues. (a) Homologues to the human CENP-M were identified in mouse (83% amino acid identity), Xenopus (57%) and chicken (41%) from existing databases.

(b) Human CENP-N contains 72%, 51% and 34% amino acid identity to the mouse, Xenopus and zebrafish homologues, respectively. Boxes indicate amino acids identical to those present in the human homologue.

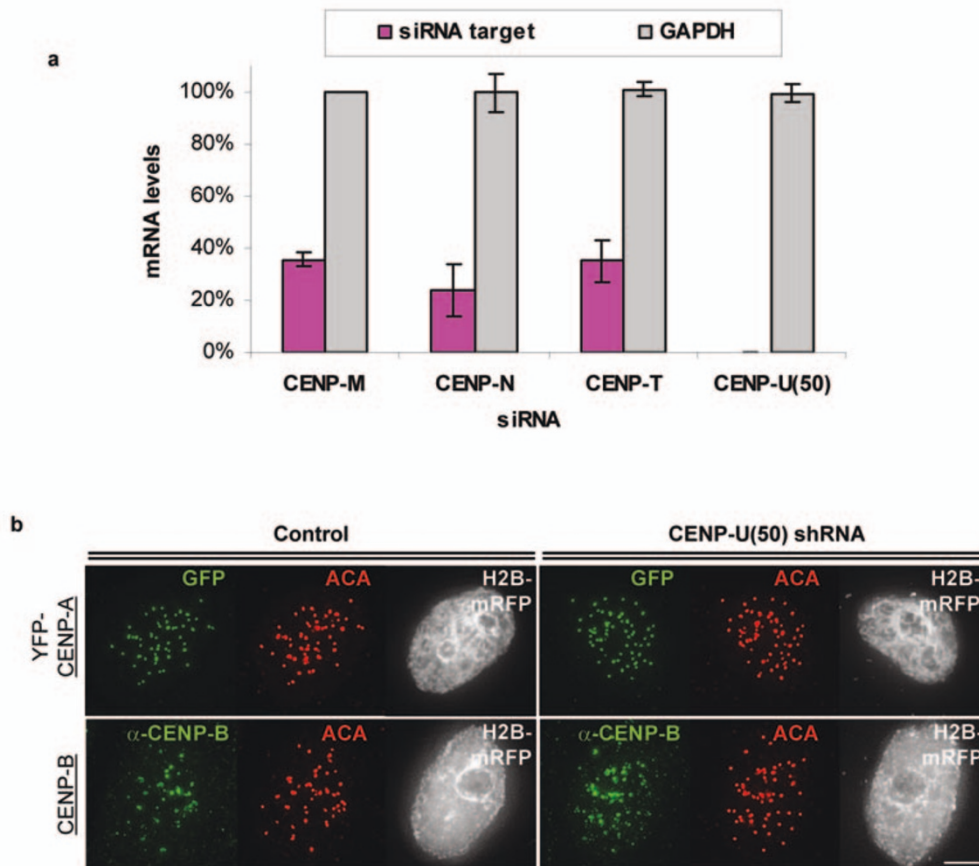


Figure S3 (a) Levels of mRNAs encoding CENP-M, CENP-N, CENP-U(50) and CENP-T after introduction of corresponding siRNAs or shRNAs assessed by quantitative PCR. Analyses were conducted in duplicate and results are expressed as the percentage of the corresponding mRNA in cells treated with control siRNA or shRNA. **(b)** CENP-A and CENP-B loading onto centromeres

assessed in wild-type HeLa cells or HeLa cells stably expressing YFP-CENP-A 72 hours after introduction of CENP-U(50) shRNA encoding vector. CENP-A was detected by immunostaining for YFP and CENP-B was detected with a CENP-B monoclonal antibody. CENP-U(50) levels at kinetochores were undetectable (as shown in Fig. 4d). Scale bar = 5 μ m

Supplementary Movie 1 Normal mitotic progression in control HeLa cells followed by cell time-lapse microscopy of cells co-transfected with a gene encoding H2B-eYFP and a control shRNA vector. Images were collected at 5 minute intervals.

Supplementary Movie 2 Multiple mitotic errors in HeLa cells with reduced CENP-U(50). Time-lapse microscopy of cells 72 hours after co-transfection with constructs encoding CENP-U(50) shRNA and H2B-eYFP was used to collect images at 5 minute intervals beginning in prophase.

Newly identified CENP proteins		
Gene Name	CENP designation	Accession No.
FKSG14	CENP-K	NP_071428
C1orf155	CENP-L	NP_201576
C22orf18(PANE1)	CENP-M	NP_076958
C16orf60	CENP-N	NP_060925
MGC11266	CENP-O	NP_077298
RP11-19J3.3	CENP-P	NP_001012267
C6orf139	CENP-Q	NP_060602
ITGB3BP	CENP-R	NP_055103
APITD1	CENP-S	NP_954988
C16orf56	CENP-T	AAH15202
MLF1IP	CENP-U(50)	NP_078905

Other associated proteins		
Gene Name	other name(s)	Accession No.
BANF1	--	NP_003851
CHAF1A	CAF1p150	NP_005474
CHAF1B	CAF1p60	NP_005432
CENP-A	--	NP_001800
CENP-B	--	NP_001801
CENP-C	--	NP_001803
CENP-H	--	NP_075060
LRPR1	CENP-I	NP_006724
DKFZp762E1312	hFLEG1	NP_060880
SUPT16H	FACTp140	NP_009123
SSRP1	FACTp80	NP_003137
HIST1H1A	Histone H1	NP_005316
HIST2H2AC	Histone H2A	NP_003508
HIST3H2BB	Histone H2B	NP_778225
HIST1H3E	Histone H3.1	NP_003523
HIST4H4	Histone H4	NP_778224
CBX5	HP1-alpha	NP_036249
CBX1	HP1-beta	NP_006798
H2AFY	Macro H2A	NP_004884
NPM1	Nucleophosmin1/B23	NP_002511
RBBP7	CAF1p46 or RbAp46	NP_002884
RBBP4P	CAF1p48 or RbAp48	NP_005601

Table S1. Summary of gene names and accession numbers of proteins identified by affinity purification.